

On the feasibility of a real time stability assessment for fishing vessels

Lucía Santiago Caamaño ¹, lucia.santiago.caamano@udc.es

Marcos Míguez González ¹, mmiguez@udc.es

Vicente Díaz Casás ¹, vdiaz@udc.es

¹ *Integrated Group for Engineering Research*

University of A Coruña, C/Mendizabal s/n, 15403 Ferrol, Spain

Corresponding author:

Lucía Santiago Caamaño

Integrated Group for Engineering Research

Escola Politécnica Superior

Universidade da Coruña

Mendizábal s/n

15403 Ferrol (A Coruña)

Spain

Telf: 34-881013864

Fax: 34-981337410

E-mail: lucia.santiago.caamano@udc.es

Link to publisher versión: <https://doi.org/10.1016/j.oceaneng.2018.04.002>

© 2018. This manuscript version is made available under the CC-BY-NC-ND 4.0 license <https://creativecommons.org/licenses/by-nc-nd/4.0/>

How to cite: Santiago Caamaño, L., Míguez González, M., Díaz Casás, V., 2018. On the feasibility of a real time stability assessment for fishing vessels. *Ocean Engineering* 159, 76–87. <https://doi.org/10.1016/j.oceaneng.2018.04.002>

1 ABSTRACT

2 Fishing is one of the sectors with the highest number of accidents worldwide. Many of them
3 are related to stability failures and affect mostly small and medium sized fishing vessels. One
4 of the main reasons is the crew lack of training in stability matters. Due to this, guidance
5 systems have emerged in the last years as a solution to this matter, complying with three main
6 requirements: being simple, being easy to use and being inexpensive to install and maintain.
7 The authors have proposed their own alternative consisting on an onboard stability guidance
8 system. However, it has some weak points. The aim of this paper is to propose an alternative
9 to overcome one of them, the need for crew interaction. In order to do this, and to try to set up
10 a fully automated system, a methodology to estimate ship's stability in an automatic and
11 unattended way based on a frequency analysis of roll motion and on the estimation of the ship's
12 inertia is presented. The results have been compared with data from a towing tank test campaign
13 showing good performance.

14

15 **KEYWORDS:** Onboard stability guidance, Fishing vessels stability, Stability monitoring

16

17

18

19 1. INTRODUCTION

20 Fishing is one of the main industrial sectors in Spain; the size of the fleet (tonnage and power)
21 and the volume of catches indicate it. At European level, the Spanish fishing fleet represents
22 the largest number of registered tons, reaching 372,617.02 GT, representing 22.46% of the total
23 value by the end of 2013, according to the European Register of Ships (Ministerio de
24 Agricultura Alimentación y Medio Ambiente, 2014). If global data are considered, Europe
25 would be located in fifth place in the ranking of fisheries production (3.4%) behind China,

26 Indonesia, India and Peru (European Market Observatory for Fisheries and Aquaculture
27 Products, 2014).

28 Regarding the technical aspects of the fishing vessels, the main characteristic of this fleet is
29 that it is very heterogeneous. There are many different typologies of fishing vessels depending
30 on their size, fishing distance to the coast, type of fishing, etc. However, two main groups may
31 be defined, according to their operation model: coastal-artisanal fleet and industrial fleet. The
32 first group is characterized by vessels with a low degree of mechanization and specialization
33 among crew members. Productivity depends on human strength and the workers' skills. The
34 number of crew members rarely exceeds 10 people and the vessels fish close to their base port.
35 The industrial fleet consists of deep-sea fishing. The vast majority of vessels exceed 24 meters
36 in length and fish far from their base port. The degree of mechanization and specialization of
37 the crew is high and the number of crew members ranges between 12 and 60 (Álvarez-
38 Santullano, 2014). The total number of fishing vessels in the world is about 4.36 million; from
39 these, more than the 85% of the engine-powered fishing vessels are less than 12 meters in
40 length, a 13% are between 12 and 24 meters length and only a 2% are over 24 m
41 (Gudmundsson, 2013).

42 On the other hand, fishing has been, and continues to be, one of the most hazardous occupations
43 worldwide. In 2001, the International Labour Organization estimated about 24,000 fatalities
44 per year and in many countries, such as Spain, USA or UK, fishing has one of the highest fatal
45 injury rates in comparison with the rest of the sectors (Bureau of Labor Statistics, 2014;
46 Ministerio de Empleo y Seguridad Social, 2013; Petursdottir et al., 2001; Roberts, 2002). Most
47 frequent accidents include the incorrect operation of the ship, modifications of the weight
48 distribution of the vessel, sailing in very adverse weather conditions that can lead to foundering
49 or capsizing or a combination of all of them. Despite of the fact that capsizing is a rare event
50 at sea, it is one of the main causes of loss of human life and fishing vessels. Capsizing is usually

51 related to stability failures, both static and dynamic (Krata, 2008; Míguez González et al., 2012;
52 Roberts, 2002; Wolfson Unit, 2004).

53 The aforementioned accidents mostly affect small and medium length fishing vessels (Krata,
54 2008; Míguez González et al., 2012) and the main reason is the crew lack of training in stability
55 matters. Only few fishermen have a deep knowledge of ship stability, especially in small-
56 medium sized fishing vessels. They usually carry out a subjective analysis to determine the
57 ship's stability level based on their previous experience. In fact, the only objective information
58 available onboard is the stability booklet. However, this has shown to be quite useless and
59 unpractical. On one hand, because of its complexity. And on the other, because it is only
60 mandatory on those ships of more than 24 m length. If this lack of training and information is
61 put together with the huge economical pressure over fishermen, one of the main causes of the
62 high accident rate affecting these vessels could be explained (Míguez González et al., 2012;
63 Petursdottir et al., 2001).

64 Having being recognized as a principal cause of accidents, both stability and operational
65 guidance have been a main research topic in the last years. Onboard guidance together with
66 training programs, provides masters more information to complement their knowledge and to
67 carry out an objective analysis of the risk level of their ships, minimizing this probability of
68 accident (Deakin, 2005; Marine Accident Investigation Branch (MAIB), 2008; Varela et al.,
69 2010).

70 In order to improve the performance of these stability guidance systems, there are some main
71 premises that have to be fulfilled. These are ease of use and understanding, low cost of
72 acquisition, installation and maintenance and minimum need for crew interaction (Deakin,
73 2005; Womack, 2003). The first approach to these kind of systems was proposed by Koyama
74 in 1982, who used a pendulum for estimating the roll period and the safety level of the vessel
75 (Varela et al., 2010). The proposal of Köse in 1995 consisted in using sensors for providing

76 weather data and applying these data for analysing the risk of capsizing of the vessel (Varela
77 et al., 2010). In 2001 Womack proposed a simple and fast application based on a colour coded
78 matrix, where different loading and weather conditions were included. Its main disadvantage
79 was the difficult understanding in vessel with a large number of compartments (Wolfson Unit,
80 2004; Deakin, 2005; Míguez González *et al.*, 2010, 2012). A similar approach is applied by the
81 Norwegian Maritime Directorate, which requires all small fishing vessels to carry a simple
82 poster, where some stability guidance is provided by using diagrams and a colour code (Deakin,
83 2005; Míguez González *et al.*, 2012, 2010; Wolfson Unit, 2004). Finally, the Icelandic
84 Administration has successfully applied a methodology which includes a compulsory inclining
85 test program, which in combination with real time weather data and ship specific stability-
86 related weather limitations, has largely reduced the number of accidents (Viggosson, 2009).

87 Within this framework, the authors, belonging to the Integrated Group for Engineering
88 Research, have developed their own alternative fulfilling the aforementioned premises. This
89 guidance system consists of a naval architecture software that, installed on a touchable screen
90 PC, from the hull forms and weight distribution of the ship, performs all necessary calculations
91 regarding to vessel stability, generating and displaying in a clear and understandable way the
92 current situation of the vessel and its risk levels. Crew interaction and ease of use premises are
93 dealt with by using an optimized user interface, which usability levels have been tested and
94 verified (Míguez González *et al.*, 2012).

95 However, the weak point of this system, as in most guidance systems, is that its full and correct
96 operation relies on the information manually introduced by the crew. For example, these data
97 include the weight items and their positions, the tank filling levels and the sea state.

98 The methodology presented in this work is part of the author's research in trying to minimize
99 the need for crew input in the aforementioned guidance system. In particular, its main objective
100 is to make a real-time estimation of the vessel natural roll frequency that, together with an

101 estimation of the vessel transverse mass moment of inertia and displacement, could lead to the
102 determination of the ship's initial stability in an automatic and unattended way.

103

104 2. METHODOLOGY

105 Considering the one degree of freedom uncoupled linear equation of roll motion of the ship
106 (Taylor et al., 2008),

$$(I_{xx} + A_{44}) \cdot \ddot{\varphi} + B_{44} \cdot \dot{\varphi} + g \cdot \Delta \cdot GM \cdot \varphi = M_{ox} \quad (1)$$

107 where M_{ox} is the external excitation, I_{xx} is the ship transverse mass moment of inertia, A_{44} is
108 the added mass in roll, B_{44} is the damping coefficient, Δ is the ship displacement and GM is
109 the transversal metacentric height.

110

111 From equation (1), the roll natural frequency for the case of small amplitude linear oscillations
112 could be estimated by:

$$\omega_N^2 = \frac{g \cdot \Delta \cdot GM}{I_{xx} + A_{44}} \quad (2)$$

113 And rewriting the previous formula, the metacentric height would be:

$$GM = \frac{\omega_N^2 \cdot (I_{xx} + A_{44})}{g \cdot \Delta} \quad (3)$$

114 If the Weiss formula based in the roll gyradius of the vessel (k_{xx}) is applied to obtain the
115 transverse mass moment of inertia, the GM estimation is reduced to (Krüger and Kluwe, 2008):

$$GM = \frac{k_{xx}^2 \omega_N^2}{g} \quad (4)$$

116 Considering the aforementioned formula, a real time estimation of the initial stability
117 characteristics of the vessel may be done by obtaining the parameters involved in these
118 equations: natural roll frequency (ω_N), transverse moment of inertia and added inertia ($I_{xx} +$
119 A_{44}) and ship displacement (Δ).

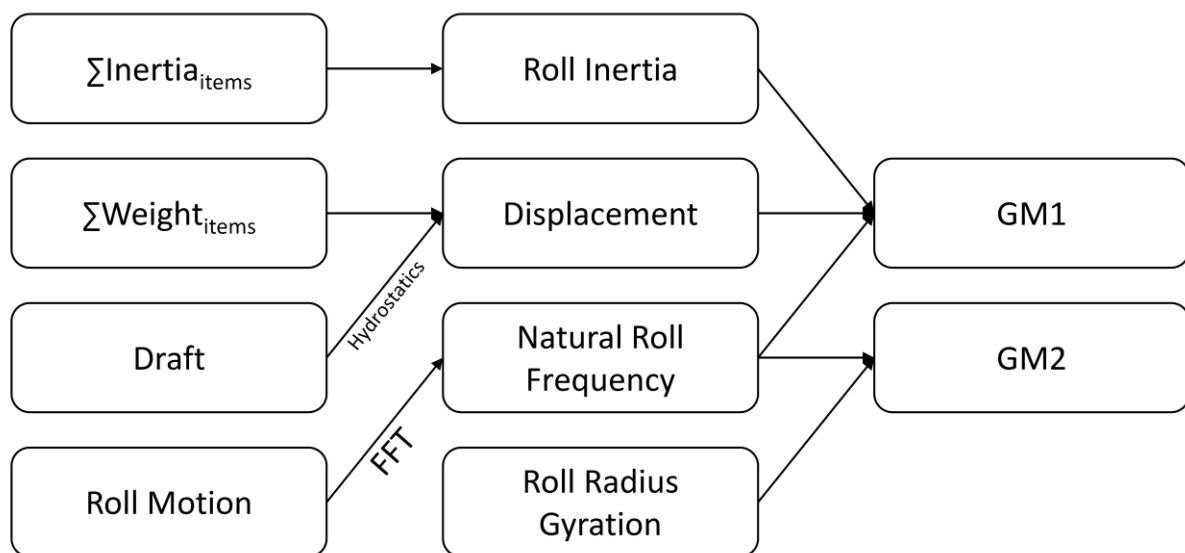
120 In this work, natural roll frequency is estimated using signal processing techniques, following
121 a procedure that will be described in the next section.

122 Regarding the transverse mass moment of inertia, two alternatives are applied. On one hand, a
123 methodology based on the approximation of the lightship mass inertia and the use of weight
124 data introduced by the crew. And on the other, the inertia is approximated using the Weiss
125 formula. In both cases, added inertia in roll is computed by using a strip theory code for
126 different vessel drafts, so the needed value is obtained by interpolation between those
127 previously computed (Neves and Rodriguez, 2006).

128 Finally, estimation of the vessel displacement is a remaining issue which will be dealt with in
129 future work. In this paper it is obtained from data which are manually introduced by the crew
130 within the system. Nevertheless, this value could also be automatically obtained using a draft
131 monitoring system.

132 Once all the variables have been obtained, the metacentric height could be estimated by
133 applying equations (3) or (4).

134 The described methodology is summarized in Figure 1.



135

136 Figure 1. Metacentric height estimation methodology.

137

138 *2.1. Roll natural frequency estimation*

139 Natural roll frequency is estimated by analyzing the roll motion and considering that its
140 spectrum has a peak around this frequency. This effect is increased when the resonance
141 phenomenon exists (Enshaei, 2013; Terada, 2014). The roll motion time series has to be long
142 enough as to ensure that it contains the minimum information needed to determine this
143 frequency with certain quality. For example, in the case of wave buoys, the length of this time
144 window is 20 minutes, as in this interval the sea is considered to be stationary. However, this
145 is too long for the case under analysis; a vessel may capsize or sink in a much shorter time, and
146 the system would not have been able to analyze the real situation and to generate an alert in
147 this conditions. The objective of a real-time stability assessment system is that the changes in
148 ship behavior could be detected, analyzed and, if needed, an alert issued, in a time window
149 long enough as to allow the crew to take corrective measures and avoid the risk situation. It is
150 generally considered (Pascoal et al., 2007; Tannuri et al., 2003) that time windows of 3 minutes
151 could be used for real time systems.

152 In addition to the above, the sampling frequency has to also comply with the Nyquist theorem
153 (Medina, 2010).

154 The power spectrum of a signal provides information about how the energy of the signal is
155 distributed into frequencies. So, from the analysis of this frequency distribution, it is possible
156 to identify the natural frequency of the system by determining the frequencies in which the
157 main peaks are located. In order to be able to compute this power spectrum, it is necessary to
158 represent the signal in the frequency domain carrying out a time-frequency analysis. There are
159 several tools to perform this transformation. However, in order to fulfill with the real time
160 premise, the Fast Fourier Transform (FFT) was chosen was chosen (Medina, 2010). To increase
161 the simplicity of the process and without degrading the results, the signal power spectrum $S(\omega)$

162 is computed by multiplying the FFT results ($g(\omega)$) by their complex conjugate and averaging
163 it. In consequence, the proposed computation is the following:

$$g(\omega) = \text{fft}(x) \quad (5)$$

$$S(\omega) = \frac{|g(\omega)|^2}{n} \quad (6)$$

164 If the FFT is applied in a finitely sampled signal, the “spectral leakage”, which is no more than
165 energy dispersion, may appear. Its main cause are the discontinuities that exist at the beginning
166 and the end of the signal and it could degrade the signal-noise ratio and mask other smaller
167 signals at different frequencies. These effects can be mitigated by applying a window function,
168 which takes the signal to zero at the ends. Windows generally cause a reduction in the accuracy
169 of the measured peak amplitude of the signal and also introduce damping. However, this is not
170 a problem in our case, as the main objective is to estimate the frequency in which the peaks are
171 located, and not their amplitude. There are numerous window functions; in this work, only
172 those which have shown to be more accurate will be used. These are Hanning, Blackman and
173 Blackman-Harris windows (Boashash, 1992; Harris, 1978; Oppenheim et al., 1999).

174

175 *2.2. Transverse mass moment of inertia and displacement*

176 Considering the shape of the vessel and the variation of its mass characteristics along the length,
177 the computation of the transverse mass moment of inertia by direct integration is not a feasible
178 alternative. The process of mass moment of inertia computation is usually simplified either by
179 reducing the ship to a single object with a known shape and constant density or by breaking
180 down the vessel into the most representative mass items and approximating them to known
181 shapes with constant density (Aasen and Hays, 2010). In this paper, the latter alternative has
182 been selected.

183 The breakdown has been done considering the steel weight, tanks and some specific and added
184 weights which have large influence in the inertia’s value. The steel weight is supposed to

185 represent the largest percentage of the inertia and it is obtained calculating the transverse inertia
186 of the amidship section and integrating it along the overall length using the hull form curve of
187 areas.

188 The inertia of the tanks is estimated approximating their shape to a parallelepiped with their
189 dimensions and with the mass manually introduced by the skipper. The relevant specific
190 weights are the engine and the fishing gear and they were estimated as parallelepipeds located
191 in their center of gravity. In addition, we have also included the weight of ice, boxes, etc. They
192 were calculated as if they were point loads and we have supposed that the transversal position
193 of the items was in the side of the vessel to take into account the most unfavorable condition
194 in the calculation of the ship's stability.

195 The other proposed methodology for estimating the transverse mass moment of inertia, is by
196 applying the Weiss formula (Krüger and Kluwe, 2008).

$$I_{xx} = k_{xx}^2 \Delta \quad (7)$$

197 Where k_{xx} is the roll gyradius, usually taken as a percentage of the vessel's beam.

198 Regarding the added mass, it has been computed by using a strip theory code, for different
199 values of the vessel draft. Intermediate values for the actual draft, are obtained by lineal
200 interpolation from the precomputed data.

201 Finally, the ship displacement can be obtained by the sum of the load items considered in the
202 calculation of the inertia which requires the crew interaction unless draft sensors are installed.

203

204 *2.3. Uncertainty analysis*

205 In order to determine the accuracy of the results, and how the errors in the estimation of the
206 different parameters affect the obtained value of natural roll frequency, and so the stability
207 levels of the vessel, an uncertainty analysis has to be carried out.

208 In the case of roll natural frequency, it was done considering that the obtained values are
209 directly measured quantities. So, following U_{95} model, as described by (Dieck, 2007):

$$U_{95} = \pm t_{95} \left[(b)^2 + (S_X/\sqrt{N})^2 \right]^{1/2} \quad (8)$$

210 U_{95} = the 95% confidence uncertainty

211 t_{95} = is a function of v and found in a Student's table. For $v \geq 30$ $t_{95} = 2.000$.

212 b = the uncertainty of the standard (at 68% confidence). It is the systematic standard uncertainty
213 of the instrument under calibration. In this case, it has been considered as the difference
214 between the mean of the roll natural frequency obtained values in the different tests and the
215 reference value of natural frequency (obtained from a roll decay test).

216 N = the number of data points in the average calibration constant or the number of data points
217 in the calibration line fit. In this case, 64 towing tank tests have been performed.

218 S_X = the standard deviation of the calibration data.

$$S_X = \left[\frac{\sum_{i=1}^N (X_i - \bar{X})^2}{N - 1} \right]^{1/2} \quad (9)$$

219 Where:

220 X_i = the i th data point used to calculate the calibration constant, i.e. the value obtained after
221 applying the proposed methodology to each test.

222 \bar{X} = the average of the calibration data (the calibration constant). Here, the average of obtained
223 values from each test.

224 N = the number of data points used to calculate S_X , in this case, the number of tests.

225 $N-1$ = the degrees of freedom for S_X .

226 On the other hand, as the GM are values obtained from the combination of other variables,
227 which have uncertainty themselves, it will be necessary to carry out an error propagation
228 analysis, as described by (Dieck, 2007). Using this error propagation analysis, besides knowing
229 the accuracy of the results, the variables that have more influence on the correctness of the

230 solution can be recognized (vessel displacement, mass moment of inertia or natural roll
231 frequency).

232 Applying error propagation to equation (3), the uncertainty of the metacentric height is related
233 to the estimated parameters by:

$$U_{GM}^2 = \left(\frac{\partial GM}{\partial \omega_N}\right)^2 (U_{\omega_N})^2 + \left(\frac{\partial GM}{\partial I}\right)^2 (U_I)^2 + \left(\frac{\partial GM}{\partial \Delta}\right)^2 (U_{\Delta})^2 \quad (10)$$

234 Where U_{ω_N} is the natural frequency uncertainty, U_I is the uncertainty of the inertia and U_{Δ} is
235 the displacement uncertainty.

236 If the Weiss formula is used to calculate the metacentric height, the uncertainty can be
237 computed by:

$$U_{GM}^2 = \left(\frac{\partial GM}{\partial k}\right)^2 (U_k)^2 + \left(\frac{\partial GM}{\partial \omega_N}\right)^2 (U_{\omega_N})^2 \quad (11)$$

238 Where U_k is uncertainty of the gyradius.

239

240 3. RESULTS

241 In order to check the proposed methodology, results from a towing test campaign of a mid-
242 sized stern trawler have been used. These tests include regular and irregular head waves of
243 different frequencies and heights. In some of the cases, parametric roll resonance took place.
244 A detailed description of these tests can be found in (Miguez Gonzalez et al., 2012).

245

246

247

248

249

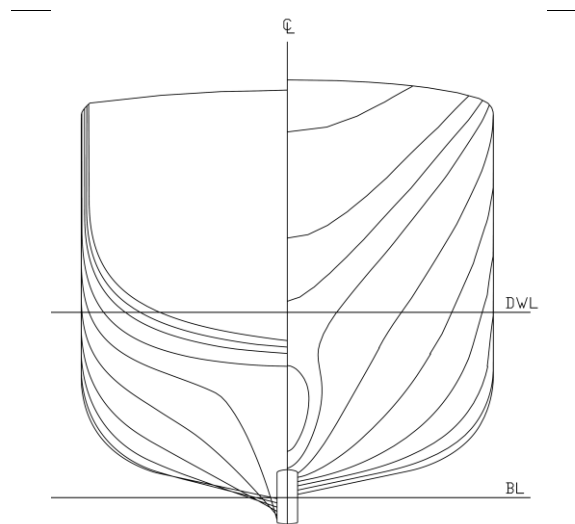
250

251

252

Table 1: Test vessel main characteristics.

Overall Length	34.50 m
Beam	8.00 m
Depth	3.65 m
Draft	3.340 m
Displacement	450 t
Metacentric Height (GM)	0.350 m
Natural Roll Frequency (ω_ϕ)	0.563 rad/s



253

254

Figure 2: Test vessel

255 The tested model is a 1/18.75 scale trawler; roll decay tests at different speeds and an inclining
256 experiment were carried out to determine the vessel metacentric height, displacement and
257 natural roll frequency, together with roll moment of inertia. These values have been used as
258 reference values. The vessel main characteristics are shown in Table 1.

259

260 3.1. Transverse mass moment of inertia

261 As it was mentioned in Section 2, the transverse moment mass of inertia was estimated
262 applying the breakdown method. The four considered loading conditions were the following:

- 263 1. Fully loaded departure. No cargo.

264 2. Fishing ground departure, 35% consumables, 100% catch.

265 3. Port arrival, 10% consumables, 100% catch.

266 4. Port arrival, 10% consumables, 20% catch.

267 The considered items and how their values in the different loading conditions are included in
268 the Table 2. In this table, the total values of the transverse mass moment of inertia of the vessel
269 resulting from applying the breakdown methodology in the different loading conditions and its
270 displacement and roll gyradius, are also shown.

271 Table 2: Dry inertia of load items considered in the breakdown methodology.

		Loading	Loading	Loading	Loading
		condition 1	condition 2	condition 3	condition 4
	Steel	3515.80	3515.50	3520.84	3570.04
	Tanks	485.73	178.80	53.43	47.93
	Fishing gear	71.473	71.71	69.40	63.17
Dry	Main engine	8.863	8.928	8.292	6.62
Inertia	Ice in hold	11.48	0.00	0.00	0.00
($t \cdot m^2$)	Fish boxes	2.30	0.00	0.00	0.00
	Fish cargo in hold	0.00	292.89	262.49	35.69
	Supplies	1.94	1.90	2.35	4.19
	Nets	346.03	344.64	358.85	404.99
<i>Total dry Inertia I_{xx} ($t \cdot m^2$)</i>		4443.61	4414.44	4275.66	4132.53
	Δ (t)	492	489	465	411
	k_{xx}/B	0.376	0.376	0.379	0.396

272 In order to check the correctness of these results, data from a roll decay test, together with those
273 from the inclining experiment, were used to determine the vessel mass moment of inertia
274 (including added inertia). From this test, natural roll frequency was obtained; added mass was

275 estimated applying a strip theory code, and the dry mass moment of inertia of the vessel was
276 subsequently computed. The obtained results are shown in Table 3.

277 Table 3: Test vessel mass distribution. Towing tank tests.

Loading condition	Δ (t)	I_{xx} ($t \cdot m^2$)	k_{xx}/B	A_{44} ($t \cdot m^2$)
Towing Tank Tests	448	4383.60	0.391	469.26

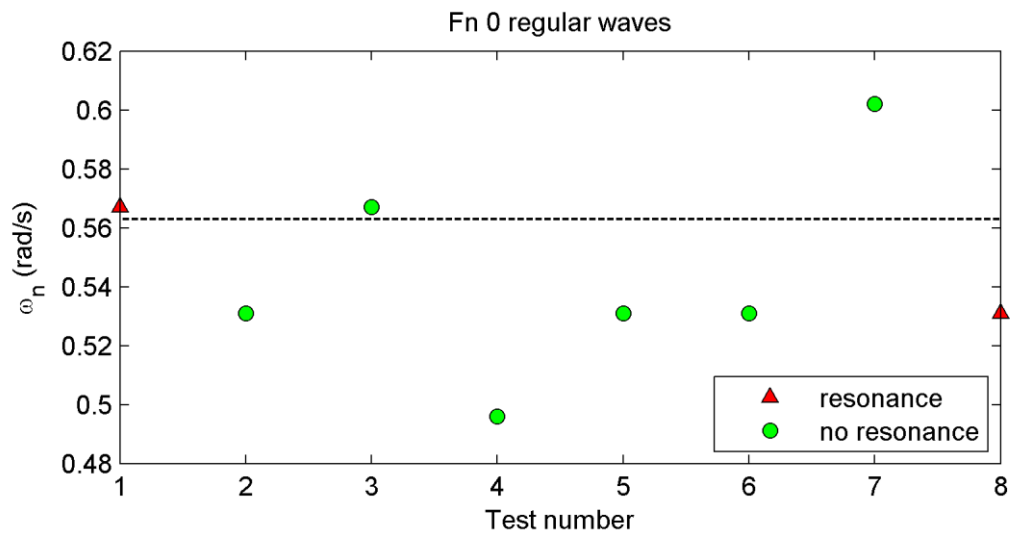
278 As it can be appreciated, the values of the dry mass moment of inertia obtained applying the
279 breakdown method are slightly different than those in the test. Likewise, the values of roll
280 gyradius are smaller than those from tests and also than the widely used reference value of 0.40
281 (Krüger and Kluwe, 2008). This difference, especially in the two arrival conditions, could be
282 explained due to the fact that in the breakdown method a more realistic distribution of the
283 weights has being done (considering cargo in holds, tanks and other weight items), which are
284 not present in the tested scale model.

285

286 3.2. Natural roll frequency

287 The results of natural roll frequency obtained in the 64 test by means of the proposed estimation
288 method are shown in the figures 3-10, separated depending on the Froude number and in regular
289 or irregular waves. In some tests resonance phenomena took place and it was represented by a
290 red triangle. When resonance does not exist, it was represented by green circles. The dashed
291 line represents the target value.

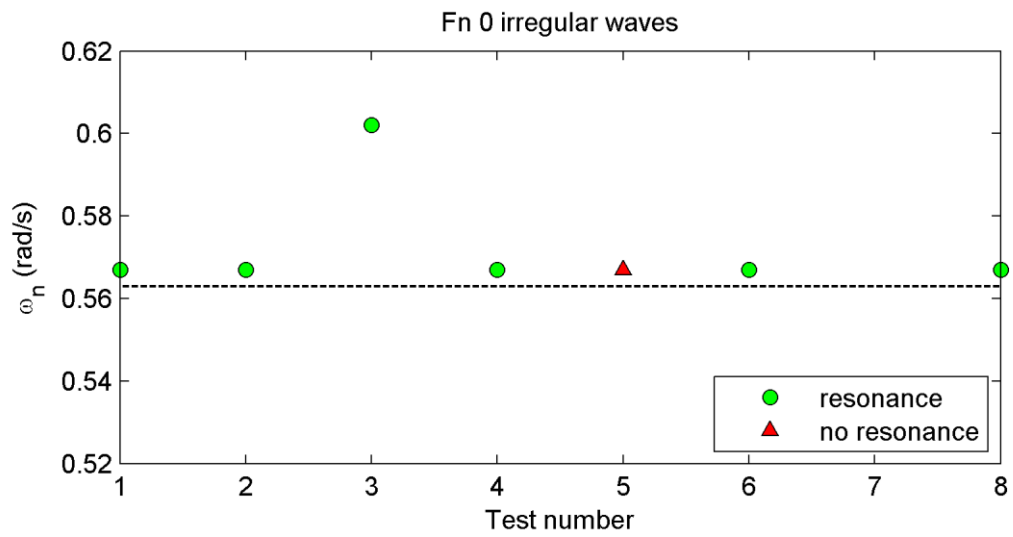
292



293

294

Figure 3. Results for regular waves and Fn 0.

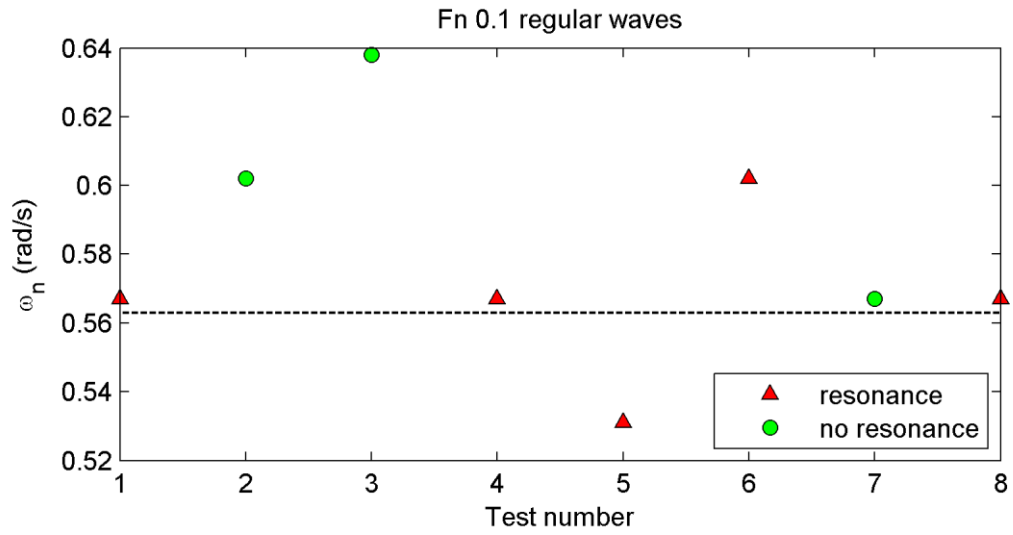


295

296

Figure 4. Results for irregular waves and Fn 0.

297

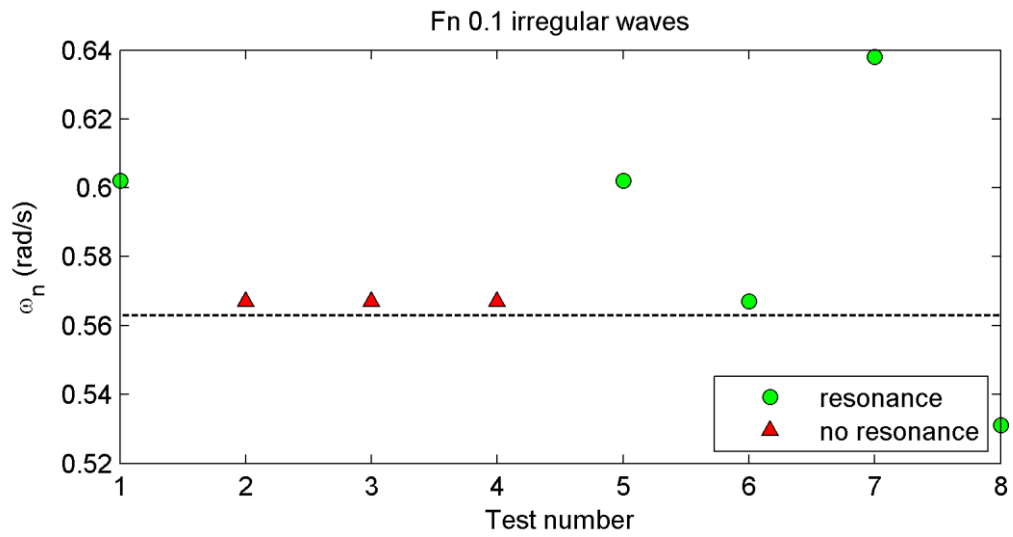


298

299

300

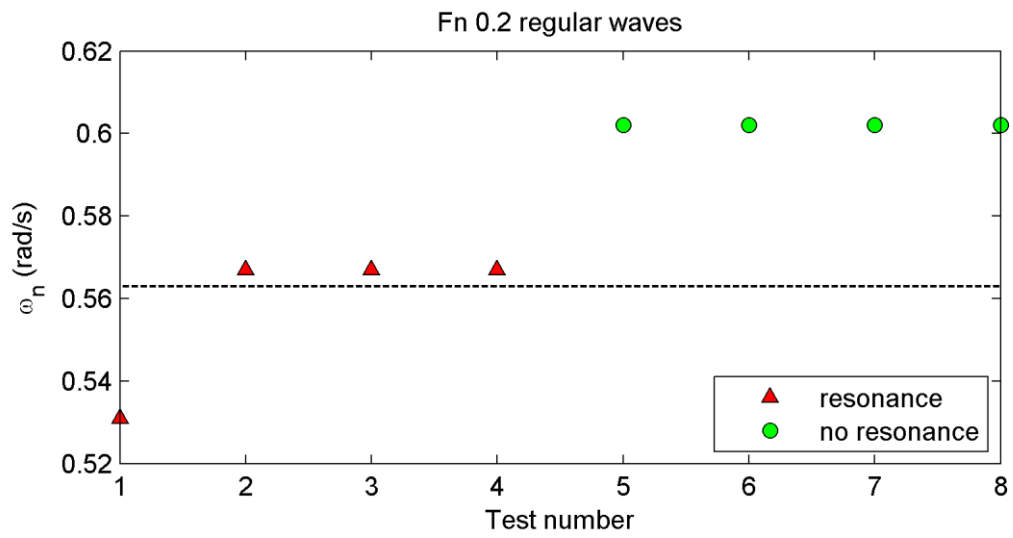
Figure 5. Results for regular waves and Fn 0.1.



301

302

Figure 6. Results for irregular waves and Fn 0.1.

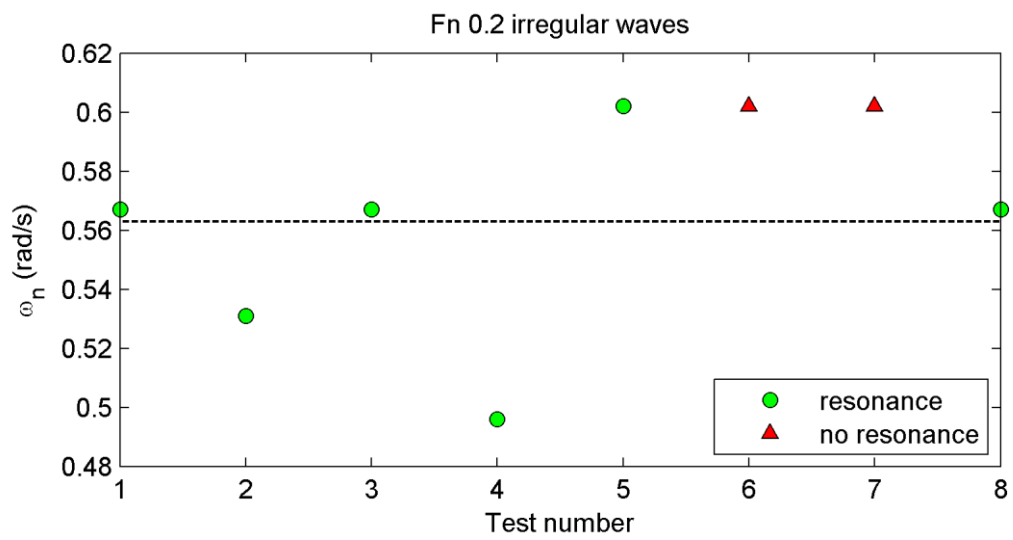


303

304

Figure 7. Results for regular waves and Fn 0.2.

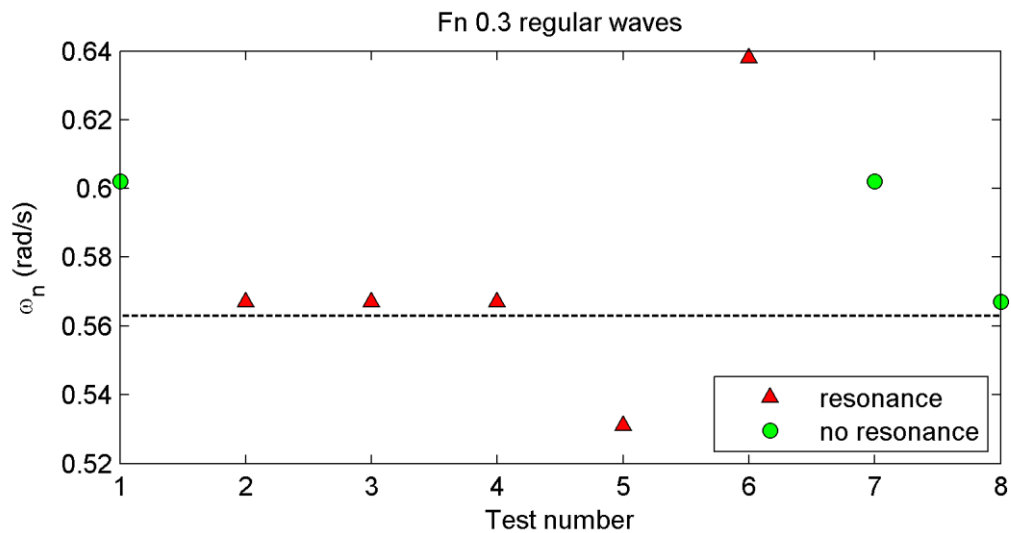
305



306

307

Figure 8. Results for irregular waves and Fn 0.2.

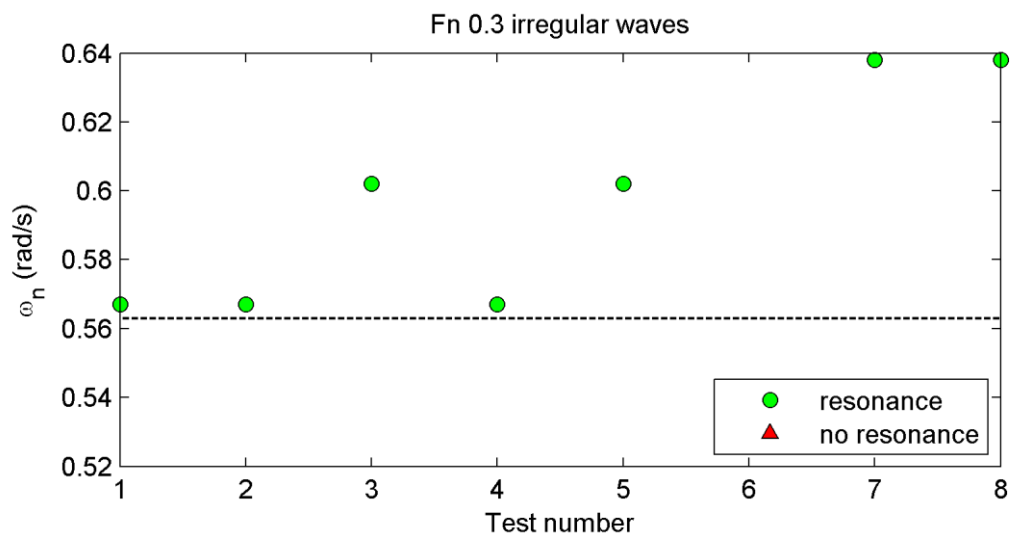


308

309

Figure 9. Results for regular waves and Fn 0.3.

310



311

312

Figure 10. Results for irregular waves and Fn 0.3.

313

314 In order to see how the estimation method works and how the use of windowing affects the

315 results of four sample cases, selected between the 64 tests already presented, are going to be

316 explained in depth. Case 1 corresponds to Test 5 in Figure 5 and Case 2 corresponds to Test 7

317 in Figure 3. Both correspond to regular wave conditions, but the first one was carried out at

318 Froude number 0.1 and the second at 0. The next two cases are in irregular waves. Case 3 is at

319 Froude number 0 and corresponds to Test 5 in Figure 4 and Case 4 is at 0.1 and corresponds to

320 Test 6 in Figure 6. . The values including the use of Hanning, Blackman and Blackman-Harris
 321 windows and the estimation of GM for each case are shown in depth in Table 4.

322 Table 4: Natural frequency results.

	Regular Waves		Irregular Waves	
	Case 1	Case 2	Case 3	Case 4
F_n	0.1	0	0	0.1
Parametric resonance?	Yes	No	Yes	No
ω_n no windowing (rad/s)	0.531	0.602	0.567	0.567
ω_n hanning (rad/s)	0.531	0.602	0.567	0.071
ω_n blackman (rad/s)	0.531	0.602	0.567	0.071
ω_n blackman harris (rad/s)	0.531	0.602	0.567	0.071
Resulting GM (no windowing)	0.311	0.400	0.355	0.355

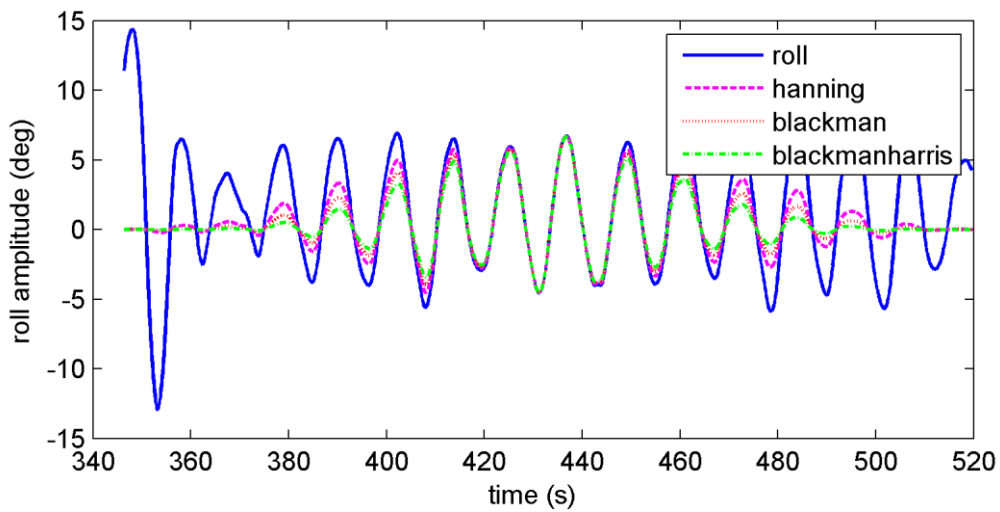
323 Hereunder, the graphical results in real scale of these tests are presented.

324 Figures 11 and 12 show the results of Case 1, a test run in regular waves where parametric
 325 resonance exists. In figure 11, the measured roll motion and the application of the window
 326 functions are presented. As it was expected, the signal is reduced to zero at the edges with
 327 windowing and its amplitude is damped. This effect is more or less pronounced depending on
 328 the type of the window used. In figure 12, the results of applying the FFT to the previous signals
 329 are included. The concentration of most of the energy of the spectrum around the natural
 330 frequency of the vessel can be seen, and is mainly due to the resonance phenomenon.
 331 Nonetheless, there is a little scattering around it, likely produced due to the discontinuities at
 332 the edges, which is less pronounced with the use of window functions.

333 Figures 13 and 14 show the results from another test in regular waves, but in which parametric
 334 rolling does not take place. This last fact makes that there is a greater dispersion of energy and

335 so, another frequency peaks have been detected. Nonetheless, a good accuracy in the result is
336 obtained.

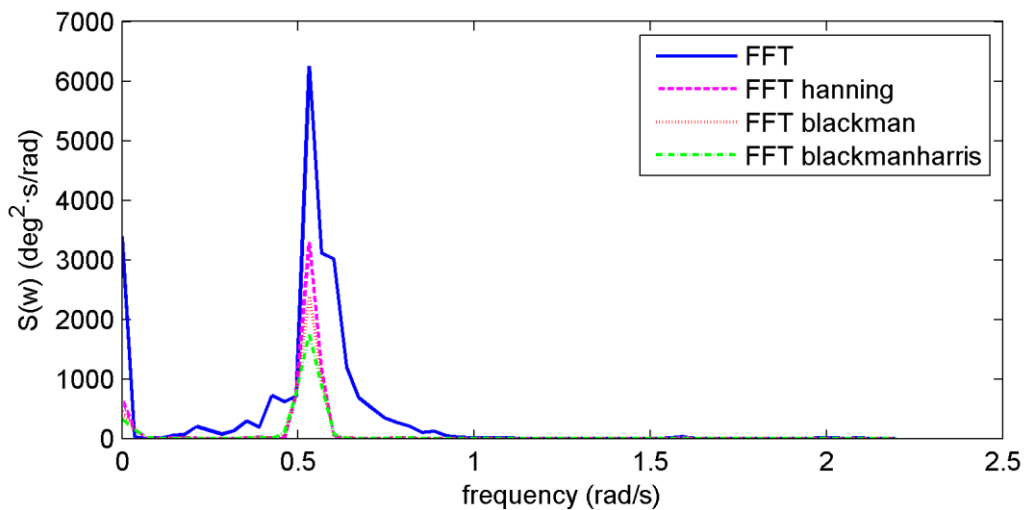
337 The other tests were run in irregular waves. When there is resonance, the energy dispersion is
338 negligible and a single peak appears in the solution (Figures 15 and 16). On the contrary, if no
339 resonance occurs, the degree of dispersion is increased, although the frequency of the system
340 can still be clearly identified except if windowing is applied (Figures 17 and 18).



341

342

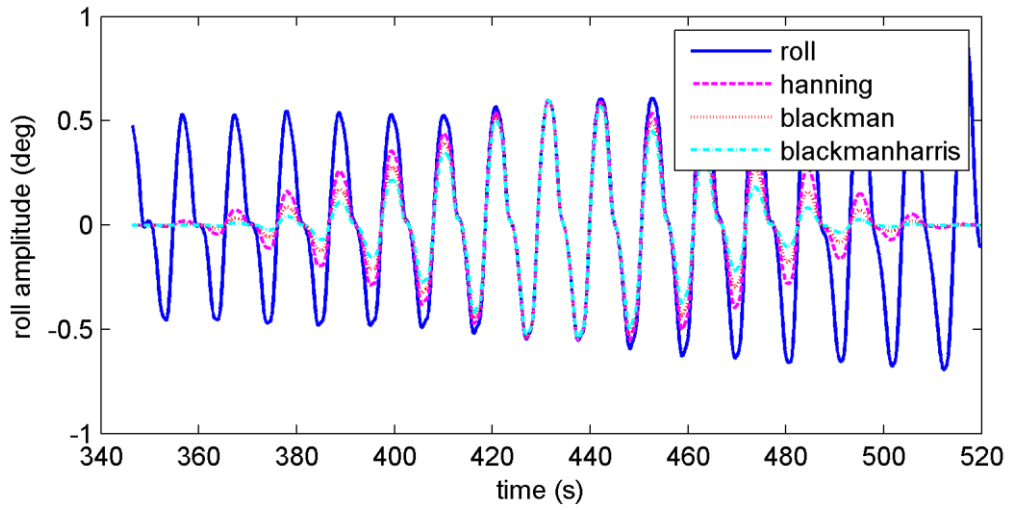
Figure 11. Case 1. Regular waves. F_n 0.1. Parametric roll occurs.



343

344

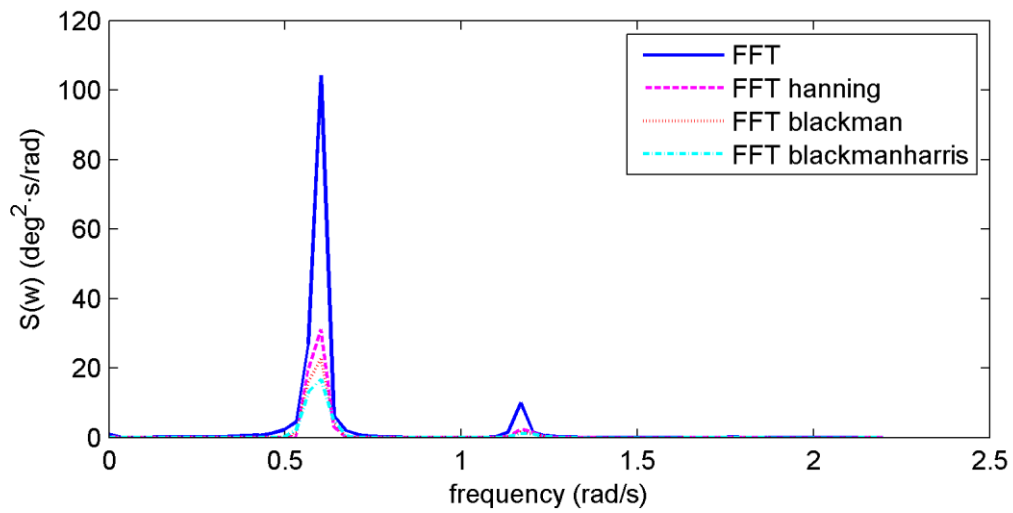
Figure 12. Case 1. Regular waves. F_n 0.1. Parametric roll occurs.



345

346

Figure 13. Case 2. Regular waves. $F_n = 0$. No parametric roll.

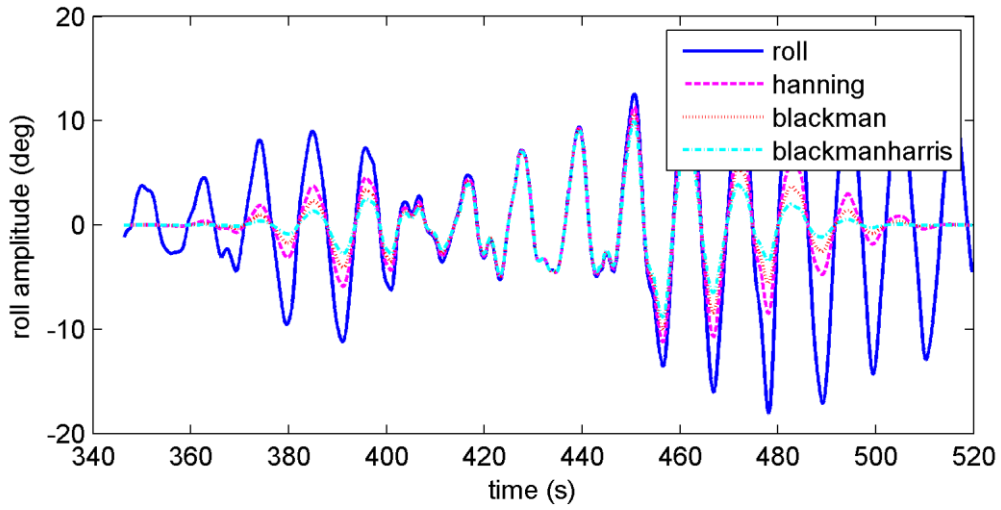


347

348

349

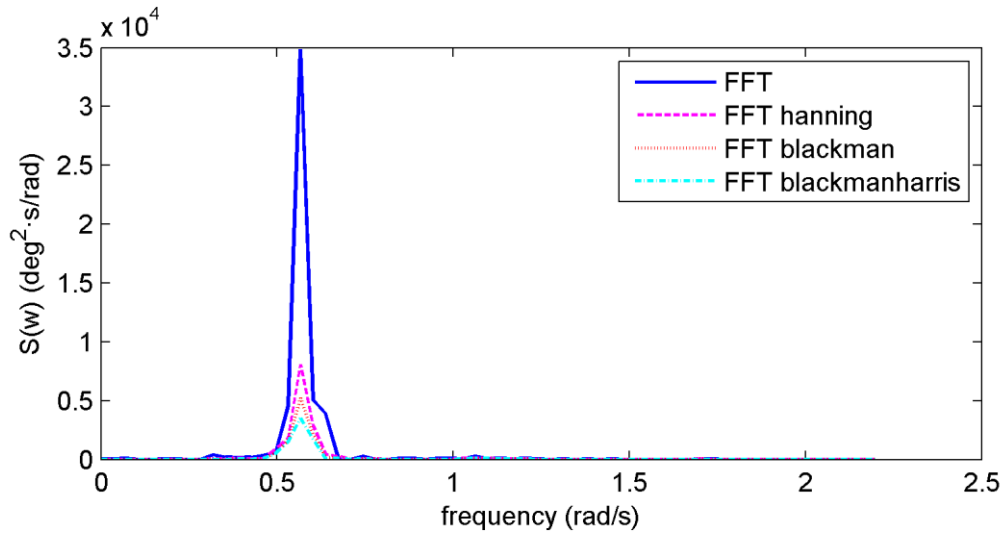
Figure 14. Case 2. Regular waves. $F_n = 0$. No parametric roll.



350

351

Figure 15. Case 3. Irregular waves Fn 0. Parametric roll occurs.

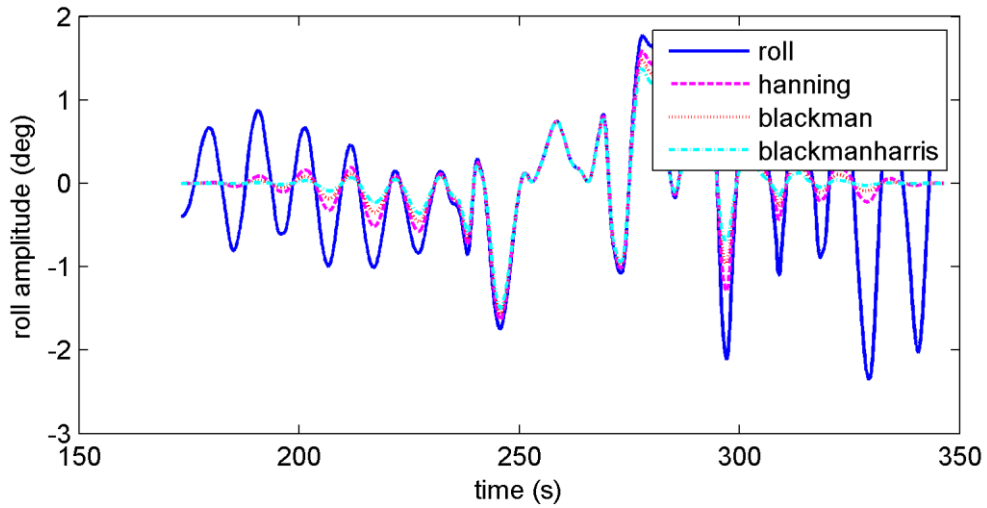


352

353

Figure 16. Case 3. Irregular waves Fn 0. Parametric roll occurs.

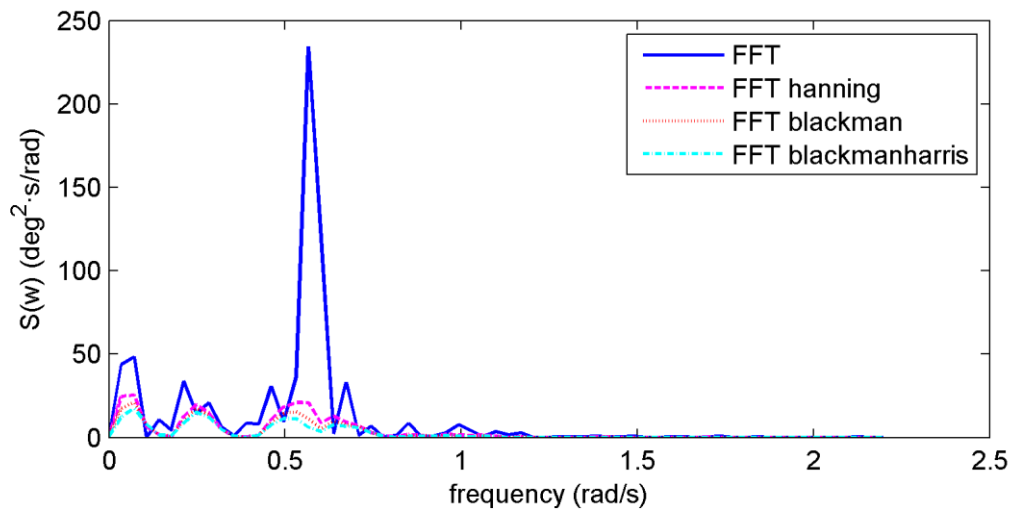
354



355

356

Figure 17. Case 4. Irregular waves. Fn 0.1. No parametric roll.



357

358

Figure 18. Case 4. Irregular waves. Fn 0.1. No parametric roll.

359 The values obtained in all the tests are very close to the actual value of natural frequency (ω_n
 360 = 0.563 rad/s).

361 The obtained uncertainty for the different values of estimated natural frequency for both
 362 windowed and non-windowed cases are shown in Table 5.

363

364

365

366

Table 5: Uncertainties in percentage of Nominal Level Units.

Uncertainty source	Systematic Standard	Random Standard	$U_{95} \pm$
	Uncertainty (b)	Uncertainty ($S_{\bar{x}}$)	
ω_n	1.857%	0.713%	3.978%
ω_n hanning	1.230%	5.426%	11.128%
ω_n blackman	0.252%	2.373%	4.773%
ω_n blackman harris)	0.043%	2.554%	5.108%

368 The uncertainty results do not exceed the 5% except in one case, so the results could be
369 considered to be satisfactory. The application of window functions showed no improvement in
370 the obtained results, being the best estimation the one obtained by the direct application of the
371 FFT and the use of no windows.

372

373 3.3. Metacentric height

374 In this section, the GM values which correspond to the natural roll frequency values previously
375 estimated, will be obtained, including the corresponding error propagation analysis.

376 The GM values corresponding to the natural frequencies obtained from the time series analysis,
377 which are shown in Table 5, have been calculated by using the real value of the mass moment
378 of inertia and displacement which were determined in the towing tank tests of the vessel.

379 If the error propagation is applied to equation (3), the values of the partial derivative terms are:

$$\frac{\partial GM}{\partial \omega_N} = \frac{2\omega_N I}{\Delta g} = 1.143 \quad (12)$$

$$\frac{\partial GM}{\partial I} = \frac{\omega_N^2}{\Delta g} = 7.470 \cdot 10^{-5} \quad (13)$$

$$\frac{\partial GM}{\partial \Delta} = \frac{-\omega_N^2 I}{\Delta^2 g} = -7.310 \cdot 10^{-4} \quad (14)$$

380 As it can be seen only the first partial derivative has a real influence in the solution, being the
381 rest of partial derivatives negligible. In conclusion, the relative error in the *GM* estimation only
382 depends in the uncertainty of the roll natural frequency.

383 As it can be seen, the weight on the solution only remains in the first partial derivative, so only
384 the uncertainty in the natural frequency has a real influence on the *GM* result. Neglecting the
385 rest of partial derivatives, the relative error in the *GM* estimation is 7.951%.

386 If we use the Weiss formula to calculate the uncertainty of the metacentric height, the partial
387 derivative terms become:

$$\frac{\partial GM}{\partial k} = \frac{2k\omega_N}{g} = 0.214 \quad (15)$$

$$\frac{\partial GM}{\partial \omega_N} = \frac{2k^2\omega_N}{g} = 1.196 \quad (16)$$

388 And the uncertainty value obtained in this case is 8.163%.

389

390 4. DISCUSSION

391 The proposed methodology to obtain the natural roll frequency has only been verified for the
392 case of head seas. If wave direction changes, the accuracy of the method is not guaranteed
393 because the forces acting on the vessel change with the wave angle of incidence and they could
394 affect the results. Thus, to extend the validity of the method to any wave direction and to
395 analyze how it performs under the different conditions it would be necessary to carry out
396 another test campaign in which following, quartering and beam seas are included as well.

397 The next point of discussion is the estimation of the transverse mass moment of inertia. By the
398 breakdown method crew interaction is still necessary. The interaction could be decreased
399 installing a remote sounding system, but the problem remains with some items as individual
400 load or cargo in hold. An alternative is proposed in this paper which consists in applying the
401 Weiss formula. This approach has two major drawbacks; on one hand this value is an estimate

402 obtained from literature. And on the other, the gyradius is kept constant for all loading
403 conditions. These two facts lead to a value of uncertainty that, although has to be taken into
404 account, it is not much higher than the one observed by applying the breakdown method. The
405 case of ship displacement is very similar to the previous one. A possible solution to avoid the
406 need of crew interaction would be to also use the Weiss formula. Another possibility would be
407 installing a draft monitoring system.

408

409 5. CONCLUSIONS

410 An alternative to overcome some of the drawbacks of the stability guidance systems for small
411 and medium sized fishing vessels has been presented in this paper. The goal is to avoid or to
412 minimize the crew interaction with the system, applying a methodology to obtain ship's initial
413 stability in real time.

414 In order to compute the metacentric height, the natural roll frequency has been estimated
415 applying a spectral analysis based on FFT to a group of roll motion time series from a towing
416 tank test campaign in head seas. The results show a good agreement with the real values,
417 considering that the uncertainty in the estimations is less than 10%. Three types of windowing
418 alternatives (Hanning, Blackman and Blackman-Harris) have been employed to try to improve
419 the accuracy of the estimation, with no success.

420 The transverse mass moment of inertia has been obtained by two different ways. The first one
421 consisted in breaking down the ship in her main load items. Data from these items have to be
422 manually introduced in the system by the crew. The second one consist on using the Weiss
423 formula to estimate the inertia, thus avoiding the need for any crew interaction. This second
424 option induces a little more error, but still the results remain satisfactory. The estimation of
425 ship displacement has been tackled in a very similar way. The crew interaction issue may be
426 overcome installing remote sounding systems and draft monitoring systems. However, and

427 considering the three initial premises of these simplified stability guidance systems, this is not
428 a feasible option.

429 In conclusion, the best option seems to be use the Weiss formula in the estimation of
430 metacentric height, at least in the case of head seas.

431

432 REFERENCES

433 Aasen, R., Hays, B., 2010. Method for finding min and max values of error range for
434 calculation of moment of inertia, in: 69th Annual Conference of Society of Allied Weight
435 Engineers, Inc. Virginia.

436 Álvarez-Santullano, F.M., 2014. Fishing effort control regulations influence on stability, safety
437 and operability of small fishing vessels: study of a series of stability related accidents
438 occurred in Spain between 2004 and 2007. Escuela Técnica Superior de Ingenieros
439 Navales.

440 Boashash, B., 1992. Estimating and Interpreting the Instantaneous Frequency of a Signal - Part
441 2: Algorithms and Applications. Proc. IEEE 80, 540–568. doi:10.1109/5.135378

442 Bureau of Labor Statistics, 2014. National Census of Fatal Occupational Injuries in 2013
443 (Preliminary Results).

444 Deakin, B., 2005. Development of simplified stability and loading information for fishermen.
445 RINA, R. Inst. Nav. Archit. Int. Conf. - Fish. Vessel. Fish. Technol. Fish. 37–46.

446 Dieck, R.H., 2007. Measurement Uncertainty. Methods and Applications, 4th ed.

447 Enshaei, H., 2013. Prevention of extreme roll motion through measurements of ship's motion
448 responses. Newcastle University.

449 European Market Observatory for Fisheries and Aquaculture Products, 2014. El mercado
450 pesquero de la UE.

451 Gudmundsson, A., 2013. The FAO / ILO / IMO Safety Recommendations for Decked Fishing

452 Vessels of Less than 12 metres in Length and Undecked Fishing Vessels – a major
453 milestone to improve safety for small fishing vessels 1–9.

454 Harris, F.J., 1978. On the use of windows for harmonic analysis with the discrete Fourier
455 transform. Proc. IEEE. doi:10.1109/PROC.1978.10837

456 Krata, P., 2008. Total Losses of Fishing Vessels Due to the Insufficient Stability. Int. J. Mar.
457 Navig. Saf. Sea Transp. 2, 311–315.

458 Krüger, S., Kluwe, F., 2008. A simplified method for the estimation of the natural roll
459 frequency of ships in heavy weather. HANSA Int. Marit. J. 9.

460 Marine Accident Investigation Branch (MAIB), 2008. Analysis of UK Fishing Vessel Safety
461 1992 to 2006 106.

462 Medina, J., 2010. Análisis de Fourier para el tratamiento de señales, in: XII Encuentro de
463 Matemáticas Y Sus Aplicaciones. Quito, Ecuador, pp. 1–39.

464 Míguez González, M., Caamaño Sobrino, P., Tedín Álvarez, R., Díaz Casás, V., Martínez
465 López, A., 2010. Un sistema embarcado de evaluación de la estabilidad y ayuda al patrón
466 de buques de pesca. Ing. Nav. 79, 90–97.

467 Míguez González, M., Caamaño Sobrino, P., Tedín Álvarez, R., Diaz Casás, V., Martínez
468 López, A., López Peña, F., 2012. Fishing vessel stability assessment system. Ocean Eng.
469 41, 67–78. doi:10.1016/j.oceaneng.2011.12.021

470 Miguez Gonzalez, M., Diaz Casas, V., López Peña, F., Perez Rojas, L., 2012. Experimental
471 Parametric Roll Resonance Characterization of a Stern Trawler in Head Seas. 11th Int.
472 Conf. Stab. Ships Ocean Veh. 625–634.

473 Ministerio de Agricultura Alimentación y Medio Ambiente, 2014. Estadísticas Pesqueras.
474 doi:10.1007/s13398-014-0173-7.2

475 Ministerio de Empleo y Seguridad Social, 2013. Estadísticas de Accidentes de Trabajo.

476 Neves, M.A.S., Rodriguez, C.A., 2006. On unstable ship motions resulting from strong non-

477 linear coupling. *Ocean Eng.* 33, 1853–1883. doi:10.1016/j.oceaneng.2005.11.009

478 Oppenheim, A. V, Schafer, R.W., Buck, J.R., 1999. *Discrete Time Signal Processing*. Book.

479 Pascoal, R., Guedes Soares, C., Sørensen, A.J., 2007. *Ocean Wave Spectral Estimation Using*

480 *Vessel Wave Frequency Motions*. *J. Offshore Mech. Arct. Eng.* 129, 90.

481 doi:10.1115/1.2426986

482 Petursdottir, G., Hannibalsson, O., Turner, J.M.M., 2001. *Safety At Sea As an Integral Part of*

483 *Fisheries Management Safety At Sea As an Integral Part*.

484 Roberts, S.E., 2002. Hazardous occupations in Great Britain. *Lancet* 360, 543–544.

485 doi:10.1016/S0140-6736(02)09708-8

486 Tannuri, E.A., Sparano, J. V., Simos, A.N., Da Cruz, J.J., 2003. Estimating directional wave

487 spectrum based on stationary ship motion measurements. *Appl. Ocean Res.* 25, 243–261.

488 doi:10.1016/j.apor.2004.01.003

489 Taylor, P., Bulian, G., Francescutto, A., Zotti, I., 2008. *Ships and Offshore Structures Stability*

490 *and roll motion of fast multihull vessels in beam waves* 37–41.

491 doi:10.1080/17445300801990913

492 Terada, D., 2014. Onboard evaluation of the transverse stability for officers based on nonlinear

493 time series modeling. *J. Marit. reserarches* 4, 31–42. doi:10.1103/PhysRevB.63.144301

494 Varela, S.M., Guedes Soares, C., Santos, T., 2010. *Monitoring System for Safety of Fishing*

495 *Vessels Subjected to Waves*. *Port. Marit. Sect.* 1–10.

496 Viggosson, G., 2009. *The Icelandic Information System on Weather and Sea State Related to*

497 *Fishing Vessels ' Crews and Stability*.

498 Wolfson Unit, 2004. *Research project 530. Simplified presentation of FV stability*

499 *information - phase 1. Final report, University of Southampton*.

500 Womack, J., 2003. *Small commercial fishing vessel stability analysis: Where are we now?*

501 *Where are we going?* *Mar. Technol. Sname News* 40, 296–302.

